Heat transfer analysis of EDM process on silicon carbide

RamezanAli Mahdavinejad
Mechanical Engineering Department, University of Tehran, Tehran, Iran
Majid Tolouei-Rad
Manufacturing Engineering Department, Shahid Rajaee University, and Tehran, Iran
Hassan Sharifi-Bidgoli
Mechanical Engineering Department, University of Tehran, Tehran, Iran

Received October 2003
Revised June 2004
Accepted June 2004

Abstract

Purpose – The purpose of the research is to analyze instability in ED machining of silicon carbide (SiC) due to heat generation in the workpiece body. The results can be used in selecting a convenient machining set up.

Design/methodology/approach – Various researches (1978-2002) have shown the importance of SiC industrial applications in many branches of technology. Instability process in EDM as a very good candidate for SiC machining is still a serious problem. Joule heating generation in SiC body due to its very high electrical resistivity is a very important point, which needs to be considered. From this point of view, the machining set up can be optimized.

Findings – The results of this research provide consideration of some factors to prevent against heat loss and voltage drop in SiC body during ED machining process. This leads the process to be more stable.

Originality/value – According to the results of this research, Joule heating due to the voltage drop in SiC body is a main factor in ED machining of this material. Therefore, some techniques as voltage injection are recommended.

Keywords Channel flow, Heat conduction, Heat transfer

Paper type Research paper

1. Introduction

Silicon carbide (SiC) is the fourth hardest material in the world only after diamond, bron nitride and bron carbide. SiC is widely used in industry since it is one of the non-oxide ceramics and has special specifications as described in Table I. High hardness, low conduction of electricity and heat, and heat shock resistance make it suitable for use in furnace as heat-element, in atomic centers as protector, and regulator of neutrons, and in machining as an abrasive material (Brook, 1991). SiC was made first in 1982 by Acheson by use of an industrial method. REFEL SiC, a special kind of SiC, has a better heat conduction due to its special production process that makes it of more widely usage.

SiC has two phases, α and β. α is cubic in low temperatures and changes to β in higher than 2,000°C, i.e. hexagonal. It melts at 2,700°C and analyses at 2,830°C (Kennedy and Shenna, 1973). In order to have REFEL SiC, a combination of α-SiC and graphite should be formed with one of the common methods. Then be sintered in

International Journal of Numerical Methods for Heat and Fluid Flow
Vol. 15 No. 5, 2005
pp. 483-502

0961-5539
DOI 10.1108/09615530510593657

Table I.
Some characteristic of steel and ceramic materials

Material	Density (g/cm^3)	Hardness (HV)	Young's modulus (E) (GN/m)	Thermal expansion 1×10^{-6}/°C	Thermal conductivity (k) at 100°C (W/m °C at 1,200°C)		Specific heat (J/g °C)	Electrical resistance (Ω cm)	Thermal shock (cal/cm s) at 500°C
REFEL SiC	3.10	2,500	413	4.30	83.6	38.9	670-710	0.42 (at 25°C) 0.016 (at 1,200°C)	59
Hot pressed silicon nitride	3.20	2,500-3,500	310	3.20	17.5	14	–	–	29
Hot pressed alumina	3.90	2,500	365	9.0	8.4	5	–	–	3
Reaction bonded silicon nitride	2.60	900-1,000	220	3.2	15	14.2	–	–	13
Tungsten carbide (6 percent Co)	15.0	1,500	606	4.9	86	–	205	20	–
Steel	7.86	800	206	12.2 (at 100°C) 13.4 (at 1,000°C)	51.9 (at 0°C)	29.7	418	1.0×10^{-5}	–

vacuumed-furnace in the presence of silicon steam. The β-SiC phase is formed, because of penetration of silicon in the body and its combination with carbon, that inhibits the α-SiC (Forrest *et al.*, 1972). SiC machining by traditional methods with regards to its high hardness is not possible (Reid and Shaw, 1969). Among non-traditional methods, electro-chemical machining (ECM) is unsuccessful because of making a very resistant oxide-layer on the workpiece. Also the electron beam machining (EBM) is not suitable because it causes powdering of operating location. Electro discharge machining (EDM) is the best method of SiC machining (Humpharey, 1976).

EDM is currently widely employed for making tools, dies and other complex-shaped parts. EDM process is based on the erosive effect of electrical discharge between the tool and the workpiece immersed in a liquid dielectric. The basic principles of the fundamental theories have suggested that the mechanism is based on a thermal conduction phenomenon governed by heat generated from arc channel and dissipated into the tool and workpiece (Tsai and Wang, 2001). As shown in Figure 1, two electrodes, tool and workpiece, are used close to each other and the space between them is filled with dielectric fluid. Interrupted sparks are made in the nearest opposite peaks and in each pulse, a small part of workpiece surface is cut. Finally, the supplementary face of tool is made on the workpiece. In this non-traditional machining method, the behavior of this semi-conductor substance is different from conductors. The majority mechanism in machining with EDM method is the thermodynamic phenomenon that is aligned with making melting spots and bulk boiling process. The high temperature gradients generated at the gap during electrical discharge machining result in large localized thermal stresses in a small heat-affected zone. These thermal stresses can lead to micro-cracks, decrease in strength and fatigue life and possibly catastrophic failure (Yadav *et al.*, 2002). Although an enormous amount of research effort has been put into representing the EDM process by experimental methods, a more elaborate semi-empirical model, based on thermal-mechanical and statistical approaches, has not yet been reported (Kulkarni *et al.*, 2002). The present paper attempts to respond this shortcoming.

2. Principles of heat conduction in EDM

Heat transfer in EDM is mostly conductive that in it a part of plasma-channel heat reaches the workpiece and almost all of this part is distributed in the workpiece by heat conduction process. Among this radiation from plasma channel to electrodes, dielectric

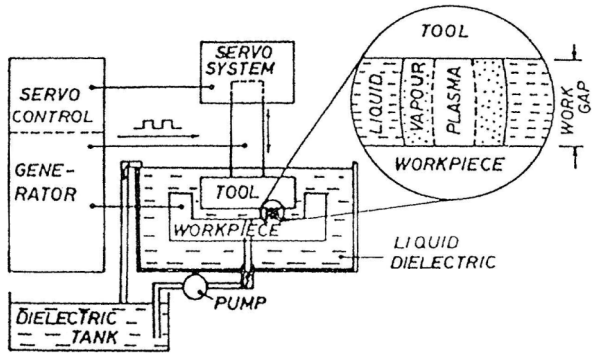

Figure 1.
Electro discharge schematic machining process

liquid and steam, radiation from electrodes to each other, also heat conduction and convection from plasma channel and workpiece to dielectric can be neglected since they are very small in comparison with heat conduction into workpiece (Van Dijck, 1973). The research undertaken by Van Dijck (1973) show that in EDM only less than 5 percent of the heat transfer is devoted to radiation. This is due to very small area of the plasma channel and very high pressure existing in this channel. The common differential equation of heat conduction in the workpiece is as follows:

$$\nabla(K\nabla T) + q^{\circ} = \rho_c \frac{\partial T}{\partial r} \tag{1}$$

where K represents heat conduction coefficient (W/m °C), q° is the rate of internal heat generation (W/m^3), ρ refers to density (kg/m^3), and c stands for specific heat (J/kg °C). In this equation, q is related to the production of heat into SiC body because of its high electrical resistance. So far various models have been used for solving this conduction equation and almost all these models were for conductive substances. And therefore, the internal Joule heat term has not been considered because of little electrical resistance. Specifically, the most important models used for solving the heat conduction equation in EDM are (Van Dijck, 1973):

(1) circular point-heat source on a semi-infinite solid;

(2) infinitely large plane heat source on a semi-infinite solid;

(3) circular heat source on an infinite cylinder;

(4) circular heat source on a semi-infinite cylinder;

(5) circular heat source on a finite cylinder;

(6) circular heat source with time dependent radius on a semi-infinite cylinder.

Among above models, model 1 has replied rather well to the very short durations of less than 0.5 s. However, it cannot be used in normal sparks, longer than 0.5 s. In model 2, the distribution of heat temperature and forecasting the boundary of melting zone is close to reality when the heat source radius is expanded or the time of spark is short and heat penetration of workpiece is low. Otherwise, this model is not precise. Model 3 is useful for specifying maximum depth of isothermals in workpiece and also, specifying the temperature of heat source center. However, it cannot be used for determining the shape of isothermal lines, melting zone boundary, and calculating the amounts of evaporation phenomenon (Van Dijck, 1973). In models 4 and 5, heat distribution in volume unit and resulting isothermal lines are more precise than other models. However, the shortcoming of these models is that heat source radius is kept constant. Model 6 is presented to deal with this shortcoming. Although similar to two latter models, model 6 is the most complete model of heat transfer since it considers the heat source radius as time dependent. Therefore, model 6 is used in this work for SiC with high electrical resistance and a considerable Joule heating.

3. Equations in circular heat source model with time dependent radius on a finite cylinder in cylindrical coordinates

In this model, the area of heat source is increased in pulse duration and as the heating flux is constant, its density is decreased (Figure 2). The differential equation of heat conduction in this model is as follows:

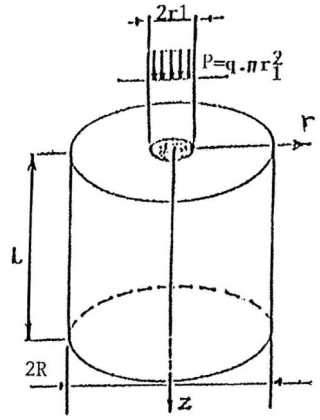

Figure 2.
Circular heat source model with time dependent radius on a limit cylinder

$$\frac{1}{r}\frac{\partial}{\partial r}\left(Kr\frac{\partial T}{\partial r}\right)+\frac{\partial}{\partial z}\left(K\frac{\partial T}{\partial z}\right)+q^{\circ}(r,z,t)=\rho_c\frac{\partial T}{\partial t} \tag{2}$$

The boundary conditions of this equation are:

$$T(R,z,t)=T_{\mathrm{o}} \tag{3}$$

$$T(r,L,t)=T_{\mathrm{o}} \tag{4}$$

$$K\frac{\partial T(r,o,t)}{\partial z}=0,\quad r>r_1(t) \tag{5}$$

$$K\frac{\partial T(r,o,t)}{\partial z}=q,\quad r=r_1(t) \tag{6}$$

And the primary condition is:

$$T(r,z,o)=T_{\mathrm{o}} \tag{7}$$

where R is the ray of cylinder of solve-field (m), L the length of cylinder of solve-field (m), T_{o} the ambient temperature (°C), $r_1(t)$ represents the heat source radius (m), and q stands for the heat flow density (W/m^2).

In this model, it is assumed that the melting and evaporation processes do not take place and the substance can be solid at more than 20,000°C. In equation (2), q is the rate of Joule heating per volume unit, and its value depends upon the coefficient of electrical resistance and current at any point in the workpiece. For determining the distribution of electrical current in the workpiece, the potential distribution should be found. This is due to the fact that, as shown in Figure 3, the current and potential lines are perpendicular to each other. Therefore:

$$\frac{\partial\rho_c}{\partial t}+\mathrm{div}J=0 \tag{8}$$

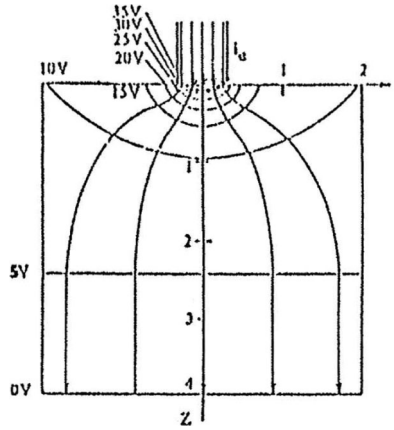

Figure 3.
Currents and potential drops in SiC bodies

As the density of charge is constant:

$$\frac{\partial \rho_c}{\partial t} = 0 \tag{9}$$

$$\mathrm{div} J = 0 \tag{10}$$

According to the Ohm rule:

$$J = gE \tag{11}$$

$$\mathrm{div}(gE) = 0 \tag{12}$$

where ρ_C is the charge density (Col./m^3), J the current density (A/m^2), g the electrical conductivity (1/Ω m), and E the electrical field intensity (V/m).

The above equation is solved by numerical method in a body graded to small elements. Therefore, all the specifications including electrical conductivity in element are supposed to be constant. In an element:

$$\mathrm{div}(E) = 0 \tag{13}$$

$$E = -\mathrm{grad}(u) \tag{14}$$

$$\nabla^2 u = 0 \tag{15}$$

In cylindrical coordinate:

$$\frac{\partial^2 U}{\partial r^2} + \frac{1}{r}\,\frac{\partial U}{\partial r} + \frac{\partial^2 U}{\partial z^2} = 0 \tag{16}$$

and its boundary conditions are:

$$\frac{\partial U}{\partial r} = 0 \quad r = R \tag{17}$$

$$U(r, L) = 0 \tag{18}$$

$$\frac{\partial U}{\partial z} = 0 \quad r > r_1(t) \tag{19}$$

$$\frac{\partial U}{\partial z} = J\rho_e \quad r \leq r_1(t) \tag{20}$$

where U and ρ_e, respectively, represent electrical potential (V) and specific electrical resistance (Ω m).

In numerical solution of this equation, although the specifications in each element are supposed to be constant, but the variation of the specifications in different elements are considered. For solving this equation we can divide the pulse duration into n steps, and in each step it is supposed that the heat source radius and physical properties are constant with respect to time. At each step the temperature of workpiece is considered the same in the whole body. Then in that step from equation (16), the electrical potential distribution can be calculated, and according to potential reduction in different regions, the rate of Joule heating per volume unit, q, is determined. Having at hand the total potential drop in the workpiece, the heat power that put by plasma on the workpiece, q, can be calculated. Having these two heat rates and using equation 2, the temperature distributions in the workpiece in this step can be determined. This cycle is then repeated until the calculated potential distribution, rate of Joule heating per unit volume, the heat power of plasma in the workpiece, and temperature distribution tend to a fixed amount. It should be noted that the acceptable tolerance amount for convergence of potential distribution is considered as 0.2 V. All these are repeated for next steps until the desired pulse duration is achieved (Figure 4).

4. Numerical solution method

For solving the differential equations of heat transfer and electrical potential, the numerical method of finite difference with central difference and explicit method is used. For this purpose, the cylindrical coordinate model has been meshed in radial,

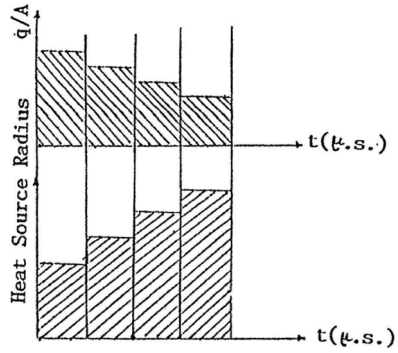

Figure 4.
Pulse dividing to time steps

vertical and surrounding directions. As these two differential equations in environmental direction are symmetric, the equations are only solved for one of the planes passing the vertical axis and cylindrical radius. The meshing is of monotonous kind and the distances between grades are equal. The form of finite difference of electrical potential is as follows:

$$\frac{1}{(\Delta r)^2}\left[\left(1-\frac{1}{2i}\right)U_{i,k}+\left(1+\frac{1}{2i}\right)U_{i+1,k}\right]+\frac{1}{(\Delta z)^2}(U_{i,k-1}-2U_{i,k}+U_{i,k+1})=0 \quad (21)$$

Also the form of finite difference of Joule heating term is as follows:

$$J_R=\frac{[U_{i-1,k}-U_{i+1,k}]}{2\rho_e\Delta r} \quad (22)$$

where J_R refers to the current density in R direction (A/m^2), and

$$J_Z=\frac{[U_{i,k-1}-U_{i,k+1}]}{2\rho_c\Delta z} \quad (23)$$

where J_Z refers to the current density in Z direction (A/m^2). Also:

$$J^2=J_R^2+J_Z^2 \quad (24)$$

$$P=\Delta V\rho_c J^2 \quad (25)$$

where P is the Joule power (W). This equation gives the rate of internal Joule heating for each network, therefore, its amount in bulk unit is:

$$q^\circ=\rho_e J^2 \quad (26)$$

By calculation of Joule heating in bulk unit and substituting in differential equations, we can obtain the explicit form of heat conduction differential equation. In this equation, which is solved for an element, the physical properties of the material are to be constant, therefore:

$$T_{i,k}^{n+1}=\frac{\alpha\Delta t}{(\Delta r)^2}\left[\left(1-\frac{1}{2i}\right)T_{i-1,k}^{n}+\left(1+\frac{1}{2i}\right)T_{i+1,k}^{n}\right]+\frac{\alpha\Delta t}{(\Delta z)^2}\left[T_{i,k-1}^{n}+T_{i,k+1}^{n}\right]+\left[1-\frac{2\alpha\Delta t}{(\Delta r)^2}-\frac{2\alpha\Delta t}{(\Delta z)^2}\right]T_{i,k}^{n}+\frac{\rho_e J^2\alpha\Delta t}{k} \quad (27)$$

$$\alpha=\frac{k}{\rho_c} \quad (28)$$

where α is the thermal diffusivity (m^2/s) and n the time index.

Equations (21) and (27) are valid for $r \neq 0$. For $r = 0$ the equations are as follows:

$$4\frac{U_{1,k}-U_{0,k}}{(\Delta r)^2}+\frac{U_{0,k-1}2U_{0,k}+U_{0,k+1}}{(\Delta z)^2}=0 \quad (29)$$

$$T_{0,k}^{n+1} = \frac{4\alpha\Delta t}{(\Delta r)^2} T_{1,k}^{n} + \frac{\alpha\Delta t}{(\Delta z)^2}\left(T_{0,k-1}^{n} + T_{0,k+1}^{n}\right) + \left(1 - \frac{4\alpha\Delta t}{(\Delta r)^2} - \frac{2\alpha\Delta t}{(\Delta z)^2}\right) T_{0,k}^{n} + \frac{\rho_e J^2 \alpha\Delta t}{k} \quad (30)$$

5. Tests performed and solution requirements

A total of 30 tests were performed on three workpieces. The specifications of workpieces, tool electrodes, machine and other equipments are described in the following sections.

5.1 Workpiece

Three SiC blocks with sizes of $43 \times 22 \times 8$ mm, $115 \times 20 \times 9$ mm and $100 \times 25 \times 5$ mm are tested.

5.2 Tool

Thirty Copper round rods of 10 mm diameter, one for each test have been used.

5.3 Machine

Deckel CNC Spark, Model DE20, ISO frequency system with nominal open circuit voltages of 120/150/180 V, with gap control system and arc and short circuit suppression. This system can produce pulse times of 1-3,000 s, pause times of 1-500 s, and spark current of 3.5-45 A at 13 situations of selectors. In this machine, the size of control gap and sensitivity of arc and short circuit suppression are adjustable.

5.4 Equipment

- The memorable two channel 40 MHz oscilloscope, Hung Chang mark, model 5804, with area 400 V and resolution 5 mV/Div-5 V/Div.
- Pointer-digitally multimeter, Hung Chang mark-with area 200 mV-1,000 v and resolution 10 μV-1 V.
- Pointer multimeter, Tandy mark, model Micronta, with area 10 A and resolution 5 A.
- A digitally balance, model Kern s2000 with area 0.0001-200 gr and resolution 0.0001 gr.
- SEM, model Cambridge with magnification × 300,000.
- Chronometer.

5.5 Test conditions

- Dielectric: crude oil with 10-20 percent trans oil.
- Tool polarity: positive.
- Open circuit voltage: 180 V.
- The number of activated transistors: 4, 6, 8.
- Pulse and pause time: $T_1 = T_0 = 10$, 20, 40, 60, 80, 100, 200, 300, 400, 500 μs.

5.6 Solving the equations

The information needed to solve the above-mentioned equations is as follows.

5.6.1 Calculation of heating flux from plasma heat source, q

$$q = \frac{1}{2} V_{\text{dis}} I_{\text{dis}} \tag{31}$$

$$I_{\text{dis}} = \frac{V_{\text{s}} - V_{\text{t}} - (V_{\text{dis}} + V_{\text{sic}})}{R'} + \frac{V_{\text{s}}^{'} - V_{\text{t}} - (V_{\text{dis}} + V_{\text{sic}})}{R''} \tag{32}$$

where V_{dis} is the discharge voltage (V), I_{dis} the discharge current (A), V_{t} the voltage drop in transistor (V), considering $V_{\text{t}} \approx 0$, V_{sic} the voltage drop in workpiece (V), V_{s} the open circuit voltage at high level (V), $V_{s}^{'}$ refers to the open circuit voltage at low level (V), R' the equivalent resistance in high level voltage (Ω), and R'' represents the equivalent resistance in low level voltage (Ω).

The equivalent resistance can be obtained from characteristics of machine pulse generation circuits in its catalogue. The open circuit voltage and the sum of spark voltage and voltage drop in workpiece are measured directly by oscilloscope during machining (Table II). For example, the calculation of the mean discharge current when four transistors are activated is as follows:

$$R' = \frac{1}{\sum \frac{1}{Ri}} = \frac{1}{\frac{3}{12.5}} = 41.67\,\Omega \tag{33}$$

$$R'' = \frac{1}{\sum \frac{1}{Ri}} = \frac{1}{\frac{1}{15.4} + \frac{1}{12.5} + \frac{1}{8} + \frac{1}{10}} = 2.69\,\Omega \tag{34}$$

$$I_{\text{dis}} = \frac{70 - 57}{2.69} + \frac{216 - 57}{41.67} = 7.90\,\text{A} \tag{35}$$

5.6.2 Calculation of heat source ray. The variation mechanism of heat source radius with discharge time is one of the most important factors in this model. To determine this radius, the microscopic pictures of melting spots obtained from SEM are used. Therefore, the picture area was divided into the spot numbers according to scale factor, and from this area the radius of melting spots is calculated (Figure 5). The variation of heat source radius with pulse duration, by using ten pictures related to ten discharge times in three adjusted situations of transistor is obtained (Figure 6).

5.6.3 Physical specifications of workpiece. In the process of solving the obtained equations, the physical specifications of workpiece such as heat conduction coefficient, density, specific heat and electrical resistance coefficients are required. These specifications are all temperature dependent but among them, changes of density and specific heat as compared with temperature are very small, and so are supposed to be constant. But the specific electrical resistance and heat conduction coefficient are extremely dependent on the temperature and by use of experimental curves (Figures 7 and 8), therefore:

$$K(T) = 970(74 + T)^{-0.45} \tag{36}$$

$$\rho_{\text{e}}(T) = 0.0045 \exp(-0.0028\,T) \tag{37}$$

No. of transistors	Material	OP.C. voltage (V) High	Low	$V_{dis}+V_{sic}$ (V)	Req (Ω) Low[a]	High[a]	V_{dis} (V)	V_{sic} (V)[b]	$I^{c}_{dis(A)}$	η^{b}	Plasma Rad (μm)[d]	$\frac{1}{2}V_{dis}I^{b}_{dis}$	I_{dis} V^{b}_{sic}
4	Silicon carbide	216	70	57	2.69	41.67	31.4	25.6	7.90	163	135	124.1	202.2
	Steel	216	70	32	2.69	41.67	32	–	18.5	–	220	296	–
6	Silicon carbide	216	70	60	1.52	41.67	31.8	28.2	9	177	144	143.1	253.8
	Steel	216	70	32	1.52	41.67	32	–	29.40	–	330	470	–
8	Silicon carbide	216	70	62	1.06	41.67	33.5	28.5	9.36	170	150	156.8	266.8
	Steel	216	70	32	1.06	41.67	32	–	40.30	–	450	645	–

Notes: [a]Measured and calculated; [b]calculated by solving deferential equations; [c]calculated from equation (10); and [d]calculated from-microscopic pictures

Table II.
Open circuit voltage, voltage dropped and resistance of power transistors

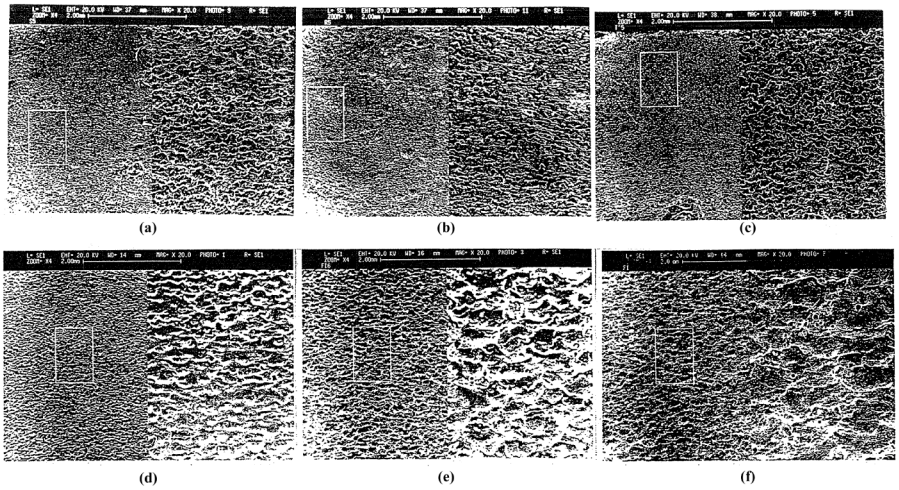

Figure 5.
Melting zone in EDM of SiC (a, b, c) and steel (d, e, a, f): (1) by 4 transistors (a, d), (2) by 6 transistors (b, e) and (3) by 8 transistors (c, f)

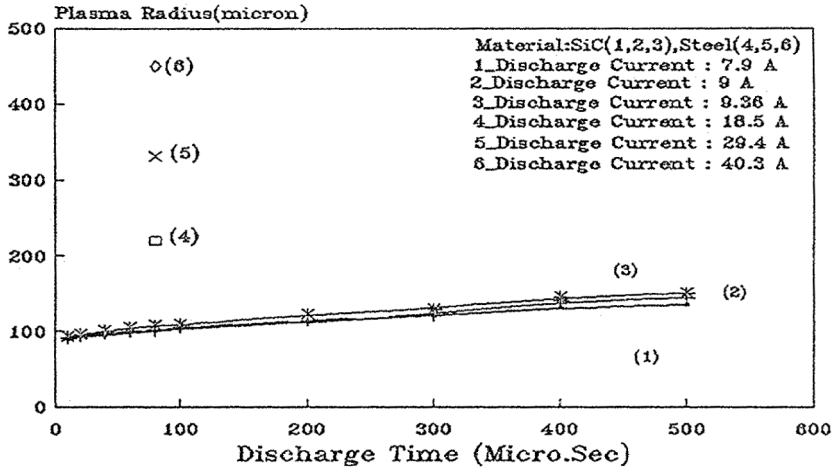

Figure 6.
Variations of plasma channel radius vs pulse times

where T is the temperature (°C), $K(T)$ the heat conduction coefficient (W/m K), and $\rho_e(T)$ the specific electrical resistance (Ω m).

5.6.4 Calculation of energy reduction percentage

$$\eta = \frac{\text{heat production in workpiece}}{\text{arrival flux of heat}} \times 100 = \frac{V_{\text{sic}} I_{\text{dis}}}{\frac{1}{2} V_{\text{dis}} I_{\text{dis}}} \times 100 = \frac{2V_{\text{sic}}}{V_{\text{dis}}} \times 100 \quad (38)$$

$$\eta = \frac{V_{\text{sic}}}{V_{\text{dis}}} \times 200 \quad (39)$$

where η, V_{sic} and V_{dis}, respectively, refer to the heat energy reduction (percent), maximum voltage at the end of pulse duration (V) and spark voltage (V)..

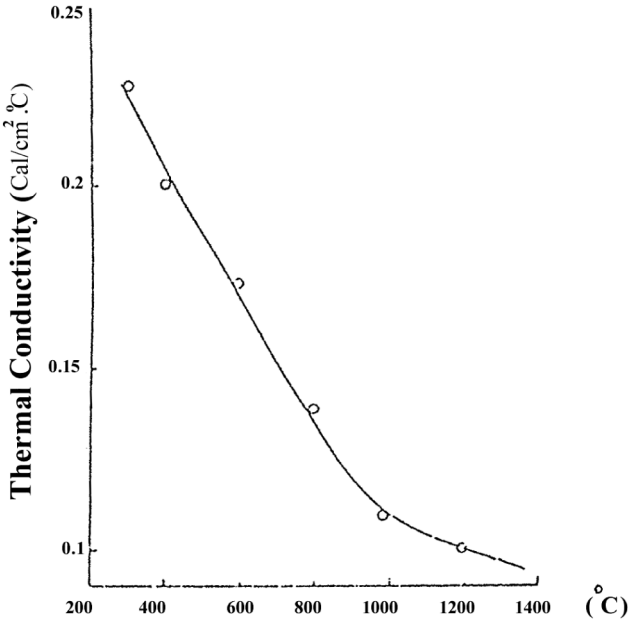

Figure 7.
Variations of thermal conductivity of SiC with temperature

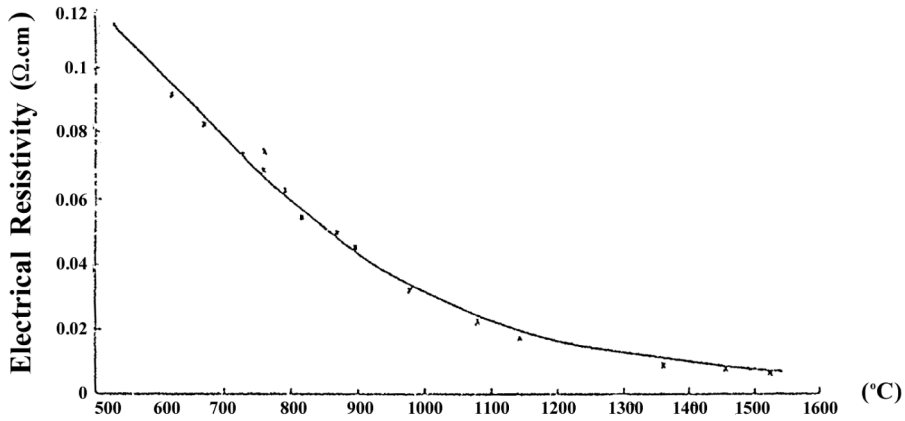

Figure 8.
Variations of electrical resistivity of SiC with temperature

6. Discussion

The loss of energy in workpiece as Joule heating is more than 160 percent of plasma energy on the workpiece (Figure 9 and Table II). This amount is produced mostly near the plasma source and the more discharge current and pulse duration, the more the Joule heating production. As can be realized, this heat is because of high voltage drop in workpiece, so that, this reduction is nearly the same as discharge voltage in the depth of 4 mm from workpiece surface (Figure 10 and Table II). The curves in Figure 9 show that in short pulse durations, the maximum rate of Joule heating production

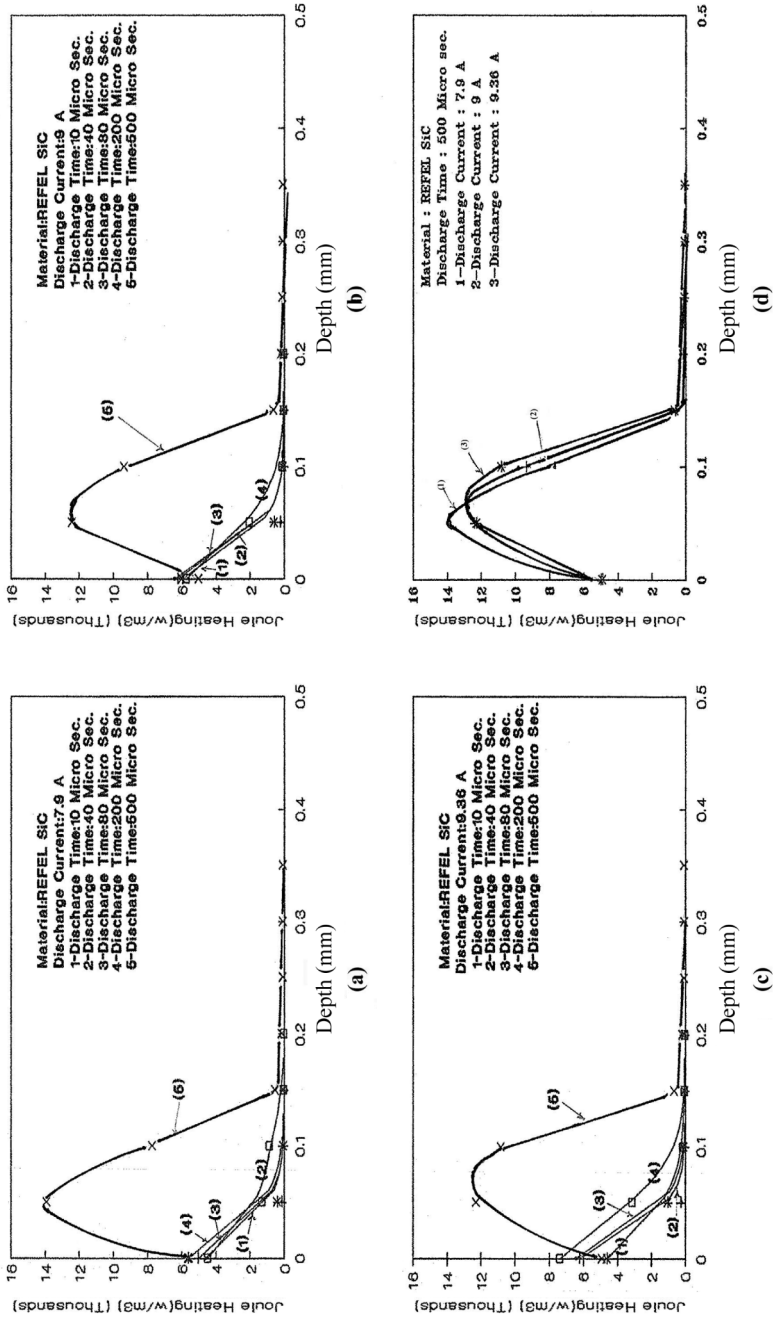

Figure 9.
Variations of Joule heating by unit volume with depth under various pulse times and currents

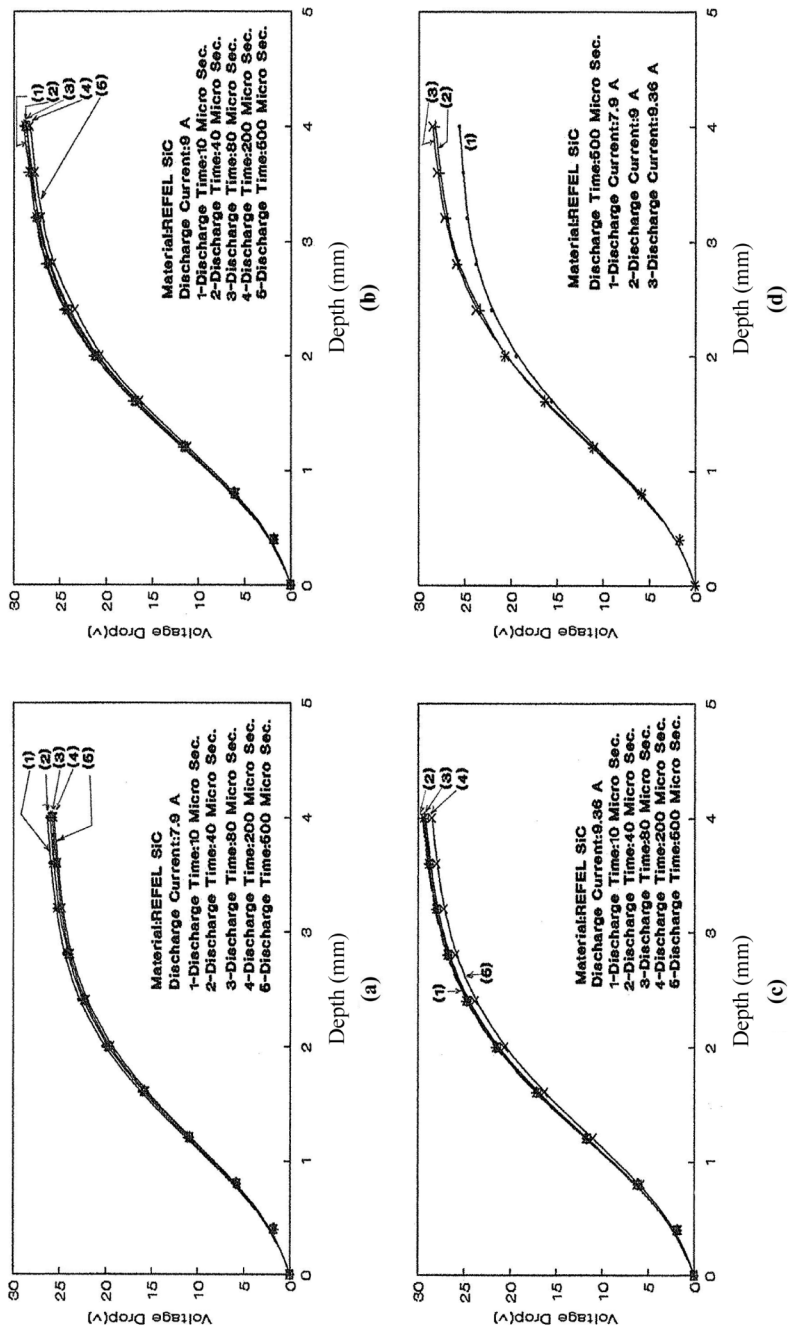

Figure 10.
Variations of voltage drop with depth in SiC bodies under various pulse times and currents

occurs on the workpiece surface, but when the pulse duration increases, the maximum is transferred below the surface layer.

The temperature distribution curves shown in Figure 11 imply that high temperature is mostly near the plasma source and it extremely decreases to the depth of workpiece such that in the depth of 0.5 mm for SiC and in a lesser depth for steel it reaches the liquid temperature. In comparison with SiC, the maximum temperature in steel is lower and the reduction intensity is less. This is shown in Figure 11(d). It can be seen from Figure 12 that most of temperature change occurs on the surface in a distance of less than 0.2 mm in steel and less than 0.4 mm in SiC from the center of spark attack. The curves in Figure 12 also show that the longer the pulse duration, the higher the maximum temperature changes and the more the radius of high temperature zone.

SEM figures taken from machining position on SiC with three different currents and its comparison with steel having similar machining conditions show that increasing current intensity does not have a considerable effect on the material removal rate. On the other hand, results obtained from the model on the same material when increasing current intensity and its effects on the surface temperature (Figure 12(d)) prove the same idea. Therefore, the experimental model is validated.

At short pulse durations, the electrical resistance and heat conduction are high and these amounts decrease as time increases (Figures 13 and 14). However, the rate of electrical resistance reduction in comparison with heat conduction reduction is less. By increasing the number of active transistors, the discharge current almost does not change, as shown in Table II. While the rate of whole Joule heating produced in the workpiece increases and reaches to the depth of the material despite increasing the number of transistors. Due to high voltage drop in the workpiece, the expansion and dimensions of melted zones do not change considerably as shown in Figure 5 and Table II. It should be noticed that in machining of steel under the same conditions, the extent of melted zone is higher and there is a considerable change with increasing the number of transistors. Reasons can be described as follows. First, as can be seen in Table I the electrical conduction of steel in comparison with SiC is very high. Therefore, the voltage drop is little and nearly the whole heat energy will be released upon arrival source of plasma. Second, with increasing the number of transistors, the discharge current increases considerably (Table II).

The heat conduction variation curve of coefficient and specific electrical resistance shown in Figures 13 and 14 indicate that changes have an increasing rate according to depth and reach the required amount in the depth of less than 1 mm. The variation temperature curve of SiC also shows that for a grading of less than 100 μm, the temperature distribution curves are almost the same (Figure 15). In solving equations, the length and width of grade is considered as 50 μm.

7. Conclusions

In EDM of SiC, the voltage drop in workpiece is very high and the same as discharge voltage. For this high voltage reduction an important part of energy in the workpiece body is wasted as Joule heating. This waste of energy reaches its maximum on the workpiece surface for short pulse durations, and near the surface in depth for long pulse durations. The temperature of workpiece is highest in the

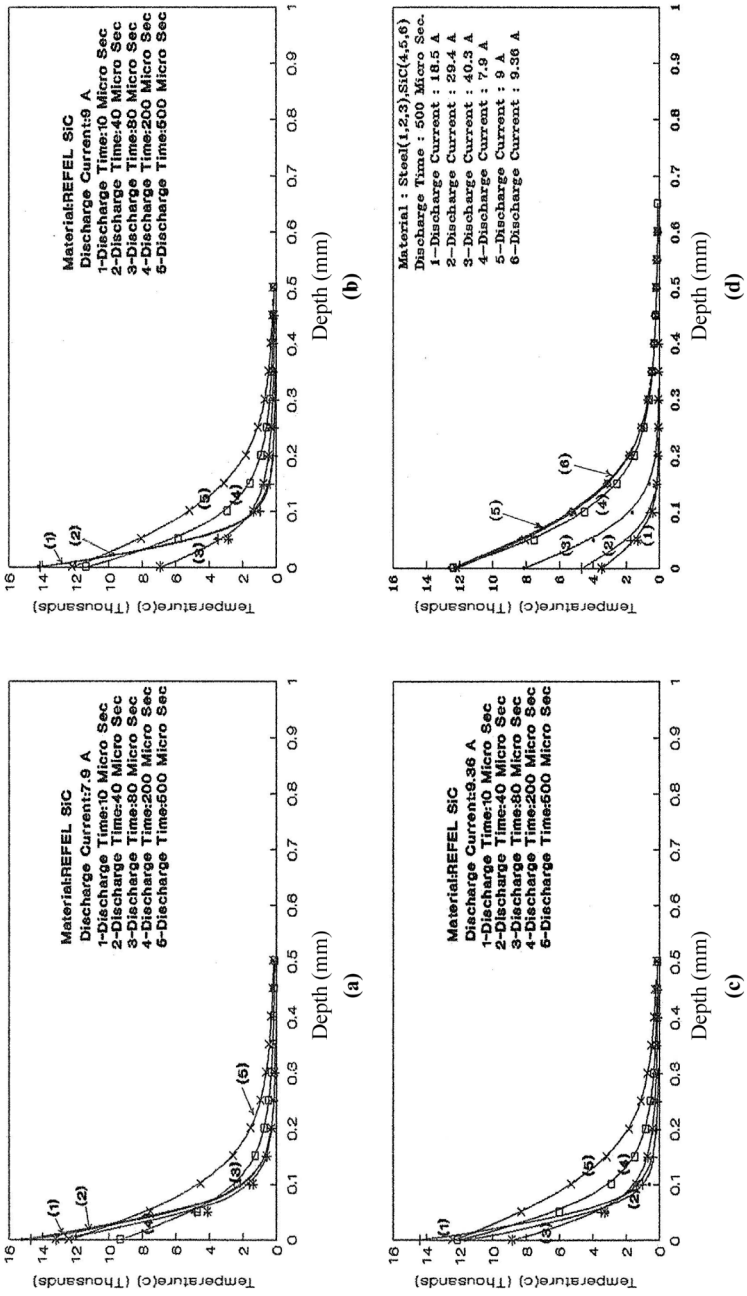

Figure 11.
Variations of temperature with depth in SiC bodies under various pulse times and currents

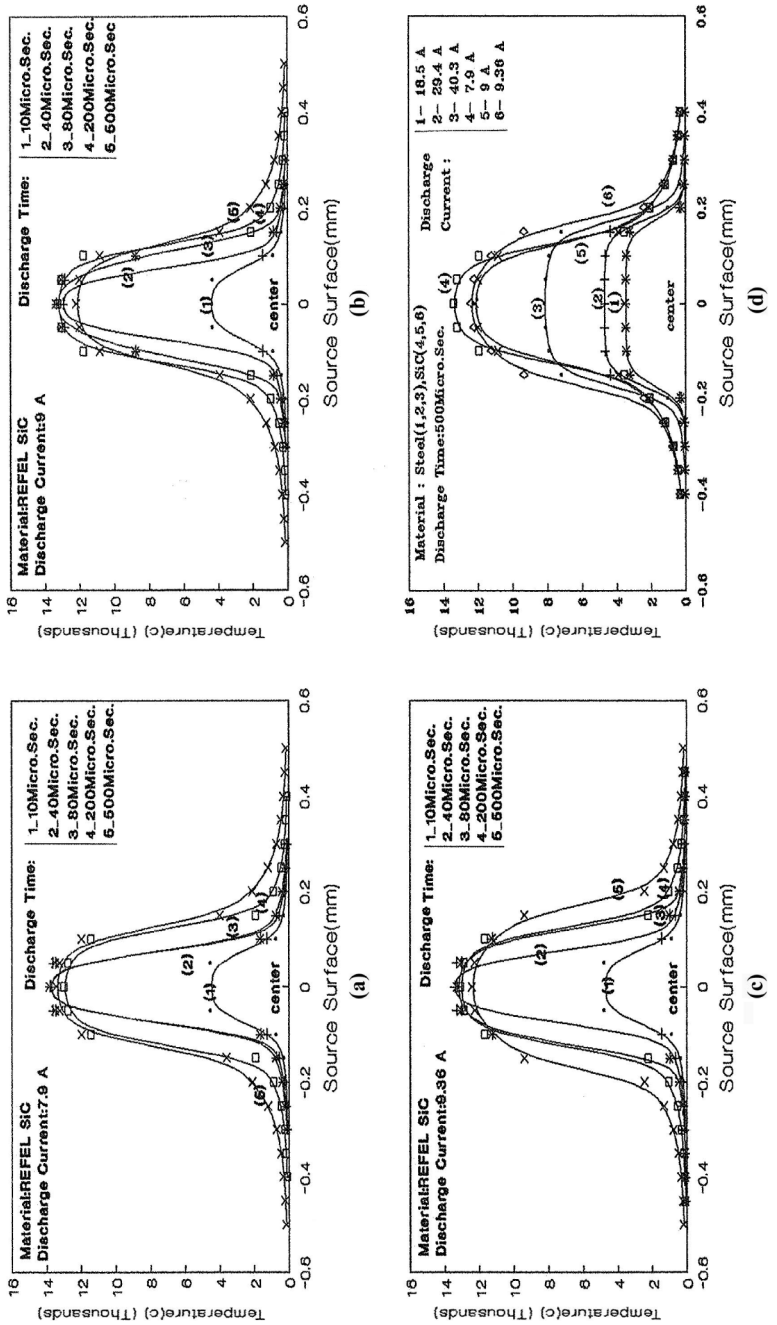

Figure 12.
Variations of SiC surface temperature with depth under various pulse times and currents

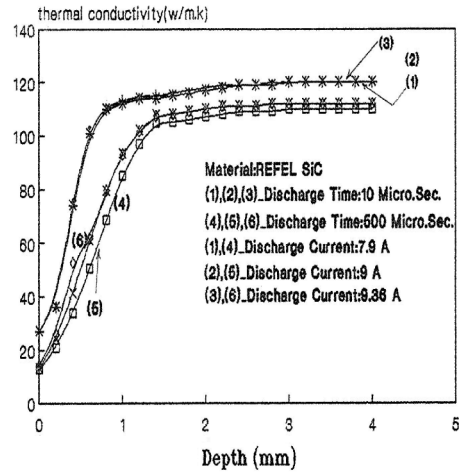

Figure 13.
Variations of thermal conductivity with depth under various pulse times and currents

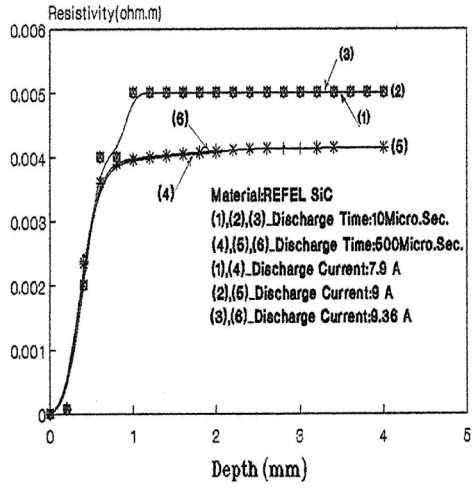

Figure 14.
Variations of electrical resistivity with depth under various pulse times and currents

center zone of spark attack and in a short distance from there in either direction, in depth and in surface, reduces rapidly. In steel, the maximum temperature is lower and its reduction in depth and surface occurs in shorter distance. An increase in the number of transistors causes more voltage reduction in SiC and a little increase in Joule heating. Discharge current and extend of melted zone does not change considerably. In comparison with SiC, the heating zone in steels is larger and with increasing the number of transistors, this area increases extremely. Solving the equations with different mesh sizes show that similar solutions are achieved when the size of grade network is below 100 μm.

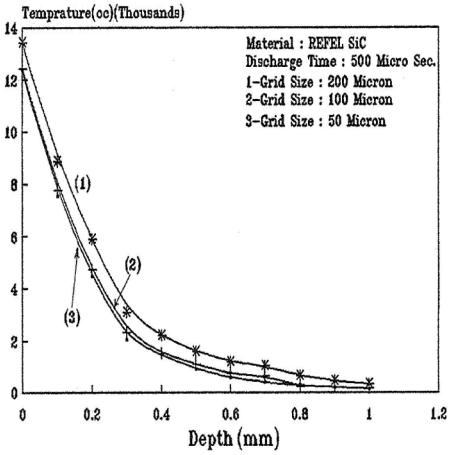

Figure 15.
Variations of temperature in SiC body with depth and various grid sizes

References

Brook, R.J. (1991), *Concise Encyclopedia of Advanced Ceramic Materials*, Max-Planck-Institut fur Metallforschung, Stuttgart.

Forrest, C.W., Kennedy, P. and Shenna, J.V. (1972), "The fabrication and properties of self-bonded SiC bodies", Special Ceramics, British Ceramic Research Association, June.

Humpharey, P.D. (1976), *An Investigation into the Electrical Discharge Machining of SiC*, Reactor Fuel Element Laboratories UKAEA, Springfields.

Kennedy, P. and Shenna, J.V. (1973), "Engineering applications of REFEL silicon-carbide", *Proceedings of 3rd Conference of Silicon-Carbide*, Miami.

Kulkarni, A., Sharan, R. and Lal, G.K. (2002), "An experimental study of discharge mechanism in electrochemical discharge machining", *International Journal of Machine Tools & Manufacture*, Vol. 42 No. 10.

Reid, D.S. and Shaw, J.W. (1969), *The Machinig of SiC*, Reactor Fuel Element Laboratories UKEKA, Springfields.

Tsai, K.M. and Wang, P.J. (2001), "Semi-empirical model of surface finish on electrical discharge machining", *International Journal of Machine Tools & Manufacture*, Vol. 41 No. 10.

Van Dijck, F. (1973), "Physico-mathematical analysis of the electr discharge machining process", PhD thesis (English translation), Catholic-University of Leuven, Leuven.

Yadav, V., Jain, V.K. and Dixit, P.M. (2002), "Thermal stresses due to electrical discharge machining", *International Journal of Machine Tools & Manufacture*, Vol. 42 No. 8.